


# ACDC: The Admixture Controlled Digital Casting and its Application to Thin Folded Concrete Structures

**Working Paper****Author(s):**

Szabo, Anna; Reiter, Lex; Lloret-Fritschi, Ena; Wangler, Timothy; Gramazio, Fabio; Kohler, Matthias; [Flatt, Robert J.](#) 

**Publication date:**

2020

**Permanent link:**

<https://doi.org/10.3929/ethz-b-000406770>

**Rights / license:**

[In Copyright - Non-Commercial Use Permitted](#)

# ACDC: The Admixture Controlled Digital Casting and its Application to Thin Folded Concrete Structures

Anna Szabo<sup>1,2</sup>, Lex Reiter<sup>2</sup>, Ena Lloret-Fritschi<sup>1,2</sup>, Timothy Wangler<sup>2</sup>, Fabio Gramazio<sup>1</sup>, Matthias Kohler<sup>1</sup> and Robert J. Flatt<sup>2</sup>

<sup>1</sup> Gramazio Kohler Research, NCCR Digital Fabrication, ETH Zurich, Switzerland

<sup>2</sup> Institute for Building Materials, NCCR Digital Fabrication, ETH Zurich, Switzerland  
flattr@ethz.ch

**Abstract.** Digital concrete technologies aim to minimize or eliminate the need for formwork, produce less waste, and build material efficient designs at increased productivity. This paper discusses how Admixture Controlled Digital Casting (ACDC) could address these aims by producing thin folded structures. For the process, a set on demand concrete composition was used to achieve minimal deformations when robotically filling weakly supported formworks. The formworks were constructed from bendable materials such as foil, geotextile or paper tensed between a frame on top and bottom and could be reconfigured for different geometries. The prototypes were assembled and post-tensioned to achieve a one-to-one scale fully functional architectural roof element. With the demonstrator presented, ACDC challenges the way we think about casting and formworks in the construction industry at the age of the 4<sup>th</sup> industrial revolution.

**Keywords:** Digital Casting, set on demand, deformations, folded structures

## 1 Introduction

Digital fabrication technologies with concrete are subject to research due to their potential to improve the efficiency and sustainability of the construction industry [1]. These novel fabrication methods aim to decrease the labour and formwork needed for concrete construction [2]. Thus, they also allow for revisiting the historical concept of folded structures providing reduced material use is combined with increased structural capacity due to its shape [3]. This paper focuses on a specific digital concrete process, Admixture Controlled Digital Casting (ACDC), as it merges characteristics of different digital concrete processes according to the need of producing thin folded concrete elements. ACDC is part of the broader family of digital casting processes [4].

ACDC uses a robotic arm to cast a set on demand material into weakly supported formworks (see Figure 2 and Section 2.1 for description of the fabrication setup). The concept for set on demand material was first applied for digital fabrication in the Smart Dynamic Casting process [5–7]. While the material is deposited by a robotic arm, similar to Layered Extrusion [8]. Although ACDC requires a formwork, with the gradual deposition and initially fluid and then fast hardening material it provides the possibility

to build it from thin, flexible or bendable materials that would burst or largely deform with traditional casting techniques (Figure 1).

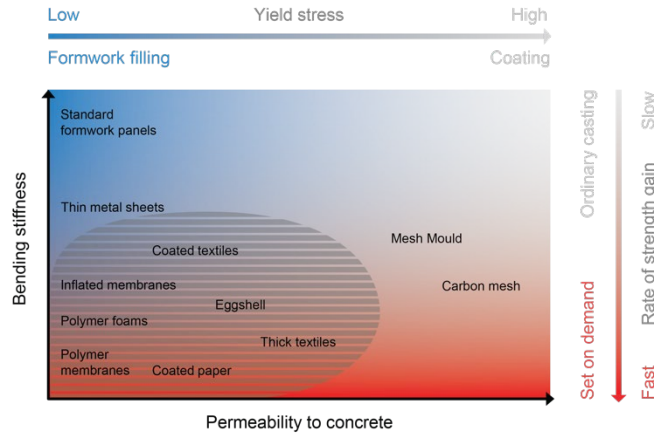


Figure 1: Possibilities of different formwork materials based on the strength evolution and rheology of the concrete filled into them. ACDC has potential in the striped zone.

Two potential set on demand mortars potentially suitable for the needs of ACDC were previously developed in lab tests and published in [9], however, those formulations had to be tested with the continuous material processing of the robotic setup discussed in Section 3.1. These initial experiments follow an experimental approach to quantify material properties, especially yield stress, and relate them to formwork deformations on a straight geometry to define the most suitable mix and fabrication parameters for the production of the large folded structure in the second experimental phase. Compared to the initial tests, the second experimental phase takes a more empirical approach to explore the influence of different formwork materials, folded geometries with changing cross-section, reinforcement integration to showcase the fabrication potential and materiality of ACDC.

## 2 Materials and methods

In this paper, two different retarded base mix formulations were tested for ACDC: an UHPC (noted ‘mix U’) with a mix design based on [10] and a self-compacting mortar (noted ‘mix S’) adjusted from previous SDC formulations [9,11]. ‘U’ comprises 0.1-0.4mm silica sand, a CEM I 52,5N Portland cement, silica fume, two types of limestone fillers while ‘S’ contains 0-4mm siliceous sand aggregates, a CEM I 52.5R Portland cement and silica fume. For both base mixes, the admixtures (sucrose 99.5% from Sigma-Aldrich as retarder and BASF MasterGlenium ACE 30 as superplasticizer) are pre-dissolved in the water and added together to the powder parts. Then ‘U’ is mixed for 10min and ‘S’ for 7min with a forced action mixer in batches of 30l.

The wet base mixes are poured into a progressive cavity pump that continuously delivers them to the mixing reactor for acceleration. ‘Mix U’ is activated with an aluminium sulfate solution with 21.4% concentration by mass. ‘Mix S’ is accelerated

with a combination of an activator (aluminium sulfate solution with 30.0% concentration by mass) and a flow enhancer (superplasticizer). The amounts are based on [9] and are represented in Table 1. The dosing happens at the robotic setup (Figure 2) by one (U\_A) or two peristaltic pumps (S\_A\_SP). The concrete dispensed by overflow from the reactor after mixing is called the accelerated concrete, the name of the accelerated mix, such as ‘S\_A\_4\_SP4.28’, indicates the activator dosage (4%) and the superplasticizer amount 4.48g/l concrete. In the second experimental phase, the superplasticizer dosage at casting slightly differs from the ones indicated in Table 1, however, the amount of addition can be seen in the mix name.

Table 1: Base mix formulations and accelerator amounts for the two mortars used here

| Retarded Mix [kg/m <sup>3</sup> ]                                     | U           |             | S           |             |
|---|-------------|-------------|-------------|-------------|
| Sand  | 616.4       |             | 1367.6      |             |
| Cement  | 547.5       |             | 615.1       |             |
| Silica fume   | 191.6       |             | 32.4        |             |
| Betocarb-SL   | 183.1       |             |             |             |
| Betoflow-D  | 419.1       |             |             |             |
| Water   | 192.2       |             | 247.2       |             |
| Superplasticizer  | 6.00        |             | 1.55        |             |
| Sucrose   | 1.33        |             | 0.68        |             |
| Ca(NO <sub>3</sub> ) <sub>2</sub>                                     | 0.03        |             |             |             |
| Accelerator [g/l <sub>concrete</sub> ]                                | U_A         |             | S_A_SP      |             |
| Al <sub>2</sub> (SO <sub>4</sub> ) <sub>3</sub> · 18H <sub>2</sub> O* | 13.7 (2.5%) | 21.9 (4.0%) | 24.6 (4.0%) | 24.6 (4.0%) |
| Water   | 50.2        | 80.3        | 57.4        | 57.4        |
| Superplasticizer**  |             |             | <b>3.45</b> | <b>4.28</b> |

\*percentage with respect to cement mass | \*\*mass of solution

## 2.1 Robotic experiments with Admixture Controlled Digital Casting

Figure 2 presents the setup for ACDC consisting of a 6-axis robotic arm (A), that is connected to a progressive cavity pump (B) at its end-effector, the mixing reactor (C), where the retarded concrete is intermixed with the accelerator dosed by one or two peristaltic pumps. Then the overflowing accelerated concrete is cast into stationary weakly supported formworks with a back and forth motion between the two ends along the straight or folded geometry (D1 and D2). The fabrication parameters such as robot speed, filling path and accelerator dosage are defined and the sensory feedback is recorded by the computer (E).

**Initial experiments.** The most suitable material composition for the continuous processing of ACDC is defined by filling straight horizontally tensed formworks with 0.5mm PVC walls and 95\*5\*40cm inner dimensions. Both base mixes and varying accelerator dosages were tested to achieve less than 15mm horizontal maximum displacement on the formwork walls. The flow rate of the mortar pump was an aggregate-size dependent constant, however, the robot speed was kept as a variable.

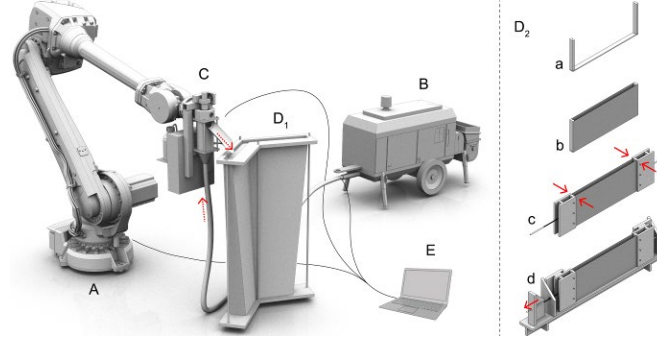


Figure 2. Robotic setup for Admixture Controlled Digital Casting (ACDC) discussed above and steps for assembling the straight formwork: a) frame, b) mounting the walls c) clamping into the holder, d) tensioning with a spring.

**Material tests.** Accelerated concrete samples were collected right before filling the formworks. Their qualitative hydration kinetics were studied with isothermal calorimetry (I-Cal8000) and their strength evolution was determined with slow penetration tests [7] using a conical penetration tip (30mm height and 10mm radius) at a penetration rate of 20mm/h with a Zwick testing machine at times presented in Table 2.

Table 2: Experiment timings and additional parameters for the initial tests

| Mix          | $v_{\text{robot}}$<br>[mm/s] | Sample<br>[hh:mm] | Slow pen.<br>[hh:mm] | Cal.<br>[hh:mm] | Grid | Force<br>sensor | Vertical building<br>rate [m/h] |
|--------------|------------------------------|-------------------|----------------------|-----------------|------|-----------------|---------------------------------|
| U_A_2.5      | 100                          | 01:20             | 01:24                | 01:28           |      |                 | 0.71                            |
| U_A_4        | 50                           | 01:11             | 01:15                | 01:19           | x    |                 | 0.71                            |
| U_A_4_rep    | 20                           | 01:25             | 01:33                | 01:37           | x    |                 | 0.71                            |
| S_A_4_SP3.45 | 20                           | 01:47             | 01:50                | 01:53           | x    |                 | 2.34                            |
| S_A_4_SP4.28 | 20                           | 01:30             | 01:38                | 01:44           | x    |                 | 2.34                            |
| S_A_4_SP4.92 | 70                           |                   |                      |                 |      | x               | 2.34                            |
| S_A_4_SP4.25 | 20                           |                   |                      |                 |      | x               | 2.34                            |
| S_A_4_SP4.42 | 20                           |                   |                      |                 |      | x               | 2.34                            |

**Deformation tests.** The deformations of the formwork walls originating in the casting process were investigated after fabrication with a dial indicator through a grid with 4\*8 measurement points (Figure 3: A). Then, continuous measurements were also performed by recording the forces with a Zemic S-type 100kg load cell at a single point in the middle of the formwork when the most suitable S\_A\_SP composition was cast at 70mm/s and 20mm/s robot speeds but constant concrete flow rate (Figure 3: B1 and B2). As a reference, this second type of measurement was repeated with a traditional wooden formwork through a hole for the sensor. On the sensor side, a 0.3mm thick PVC foil provided separation between the fresh concrete and sensor similarly to [6].

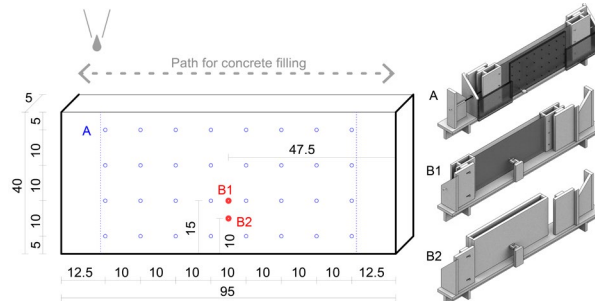


Figure 3: Deformation measurements for straight formworks with A) the front grid defining point where the displacement is measured with a hand-held dial indicator or with B) a load cell

**Folded structure demonstrator.** With the most suitable material composition (S\_A\_4\_SP4.28) and robot speed (20mm/s), the casting experiments continued with 1m tall folded formworks prepared from different light formwork materials (0.2mm PE foil, geotextile, 1.15mm RAM-board) tensioned between a lower and upper frame (Figure 4). They showed variations in fold angle and cross-section along their height thus variations in robot path and layer height were also explored. Then, they were designed as parts of a larger roof segment thus including tubes for post-tensioning cables and positioning pins acting as shear keys at the connections of the elements.

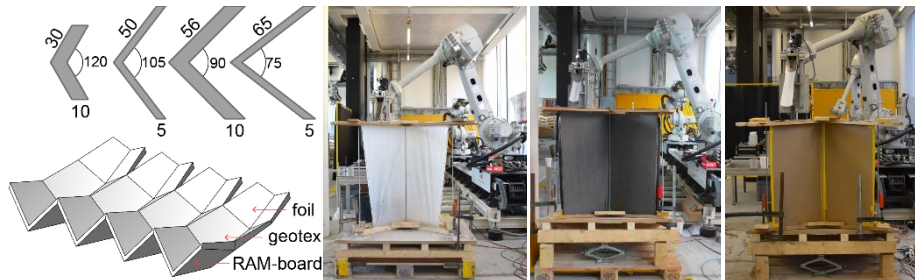


Figure 4: The design of the folded roof section with varying cross-section [cm] consisting of three elements cast in weakly supported formwork with the robotic setup.

## 3 Results

### 3.1 Initial experiments

**Material tests.** The calorimetry results are represented in Figure 5 (left). Qualitatively, a high reaction rate can be observed after activation for both U\_A\_4 and S\_A\_4 mixes (the retarded base mixes with the same composition are reported in [9]). The single hydration peaks of the U\_A samples appear at similar times even with slightly less accelerator while the silicate and aluminate reaction peaks of the S\_A\_SP mixes are

occurring later with smaller maximum when more superplasticizer is added upon acceleration.

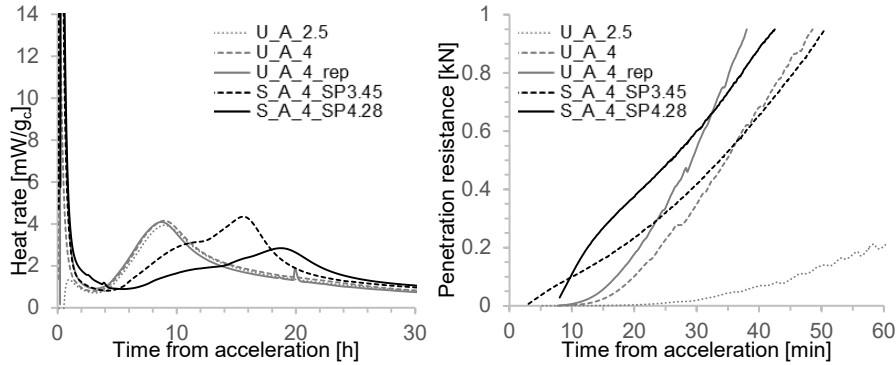


Figure 5: Evolution of U\_A and S\_A\_SP mixes with different accelerator dosages, left) Heat rate, b) penetrometer resistance.

The penetration resistance recorded with slow penetration tests in Figure 5 (right) increases with material age and more so with higher aluminium sulfate dosages for all accelerated U\_A and S\_A\_SP samples similarly as previously reported in [7,9]. The S\_A\_SP mix variants show an immediate rapid increase of penetration resistance with a lower starting point for higher superplasticizer addition while the strength build-up of the U\_A compositions is initially delayed. However, later, the strength evolution of the U\_A\_4 mixes is faster than of the S\_A\_4 mixes.

**Deformation tests.** The results of the deformation grid measurements are plotted by overlaying the coloured displacement graphs interpolated from the measurements recorded on the front of the prototypes. Thus, the filling characteristics can be observed together with the degree of deformation in Figure 7.

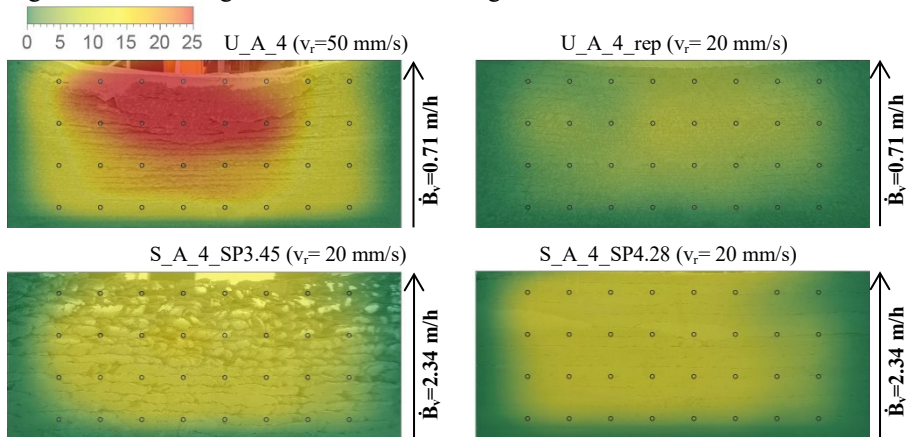


Figure 6. Grid measurements (in mm) after casting at the specified building rates

With U\_A\_2.5, the deformations were too large for the setup to detect. Regardless of the open time of U\_A\_4 after acceleration, with the low vertical building rate and slow robot speed, the deformations were minimal. Further, the deformations were at a similar range even at high vertical building rate with S\_A\_4\_SP, where the slightly increased superplasticizer addition improved the formwork filling significantly.

The results of continuous force measurements on the weak straight formworks are plotted in Figure 8, indicating the times of each robot pass with dashed lines for both robot speeds. The filling increases the load on the formwork walls even before the concrete reaches the sensor height (red dashed line). The load is higher with higher robot speed. Then the steps with which the load increases are largest around the sensor height and reach a plateau after approximately 2.5min for both samples (corresponding to 3 and 10 layers respectively with the slow and fast speeds).

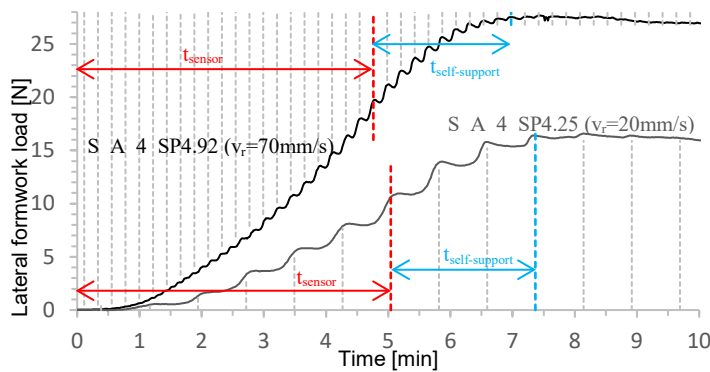


Figure 7: Forces recorded on the formwork wall during casting with different robot speeds

Compared to the weak formwork tests, with the rigid wood formwork, no significant force can be recorded before reaching the sensor height, however, the plateau appears here as well after a similar amount of time and the same amount of new layers.

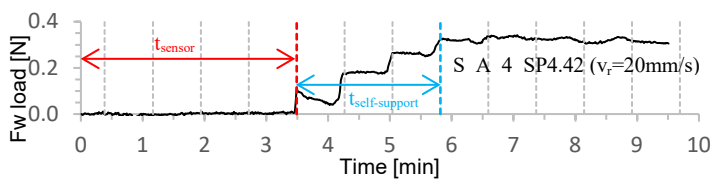


Figure 8: Forces recorded through a hole during casting into a traditional wooden formwork

### 3.2 Folded structure demonstrator

All three pieces of the demonstrator were produced successfully in the first trial and demoulded a week after. The foil formwork was easy to remove and provided a shiny smooth surface. However, the adhesion of geotextile and RAM-board on the prototype required additional effort at demoulding. Geotextile remains were brushed off without a problem and left the surface ‘furry’ while the RAM-board was washed off with high-



pressure water slightly colouring the surface and increasing the visibility of the layers. The assembly was guided by the positioning pins that showed sufficient accuracy and no cracks developed during post-tensioning (Figure 10).



Figure 9. Prototype (foil formwork) and post-tensioned folded roof section

## 4 Discussion

Qualitatively the material tests are in good agreement with the deformation tests. The high heat release in the first hour (seen from calorimetry in Figure 5) corresponds to extensive formation of hydration products responsible for rapid strength evolution (Figure 6) leading to the minimal deformations (Figure 7) during ACDC.

Figure 11 provides a graphical representation of the maximum amount of fresh layers influencing the deformations at the bottom based on the von Mises criterion. We expect that when the yield stress of the concrete is higher than half the hydrostatic pressure of the concrete above no more deformations occur. The yield stress is approximated from the slow penetration force with a coefficient of 180 Pa/N according to [9] for both U and S mortars with high accelerator dosage. The pressure due to filling increases with time as additional layers are deposited (due to the linear robot movement its steps vary at different formwork positions). Indeed, Figure 11 shows that self-support is expected for S\_A\_4 at 3min. Although it takes longer for the U\_A compositions to exceed the vertical pressure and become self-supporting, the building rate is lower, thus explaining the low deformations seen in Figure 7. The S\_A\_SP mixes reach self-support and stop deforming at a similar vertical pressure but in a lot shorter time.

The time needed to reach self-support with S\_A\_SP can also be read from the force measurements in Figure 8 and Figure 9. No additional force is recorded from the fresh concrete layers both in the rigid box and in the weak formwork after approximately 2.5mins showing good agreement with Figure 11 b. Additionally, the deformation grid could capture, but could not explain, the effect of higher robot speed disturbing the structural build-up of the previous layers resulting in larger deformations in Figure 7.

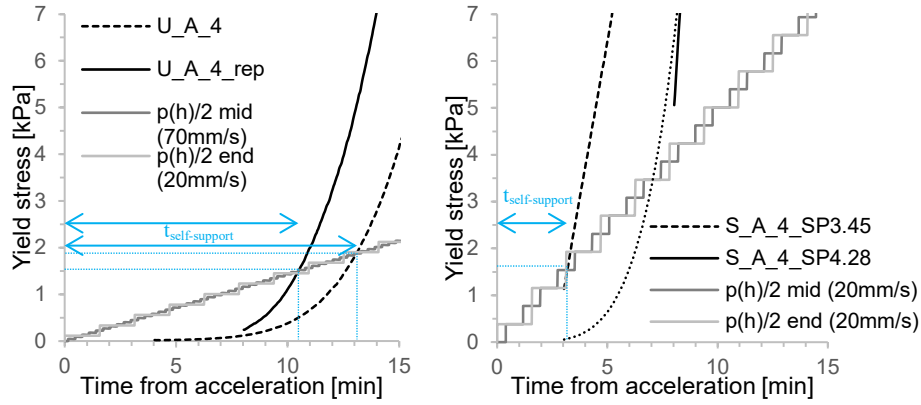


Figure 10: Comparison of yield stress evolution and hydrostatic pressure increase over time. (Unfortunately, the measurement of  $S\_A\_4\_SP4.28$  was started too late to discuss it here.)

Based on the material and deformation tests, we determined a suitable concrete composition and robot speed for the fabrication of the folded structure demonstrator. Although both mix compositions could result in low deformations, the experiments continued with  $S\_A\_4\_SP$  due to its higher vertical building rate and its robustness by the additional degree of freedom with the superplasticizer dosage. Slight changes in superplasticizer amount could compensate for day-to-day variations of the mix, different environmental conditions or changes in cross-section. Further, the lower plastic viscosity of  $S\_A\_SP$  mixes provides better formwork filling and ease of handling.

Despite the unknown exact resistance to the hydrostatic pressure of the different formwork materials, the tensioning logic between the lower and upper frame proved a successful strategy to produce one-to-one scale folded elements by ACDC. The assembly of these prototypes is a proof of concept for a system where the tolerances are low at connection surfaces, however minimal deformations are allowed leaving space for the architectural expression of ACDC from different formwork materials.

## 5 Conclusion

Digital Casting and more specifically Admixture Controlled Digital Casting (ACDC) addresses the problem of high formwork pressure with self-compacting concrete. It shows that less formwork is required by robotically casting a set on demand composition adapted to in-line continuous processing. Importantly, yield stress measurements allowed to predict the time at which self-support deformations plateaus are achieved.

Further, ACDC was robust enough to cope with the increased uncertainty of the less controlled fabrication environment shown at the production of three thin folded prototypes without the need for repetition. In summary, ACDC and more generally Digital Casting shows that formworks of the future may be light, using a small amount of potentially recycled materials instead of bulky constructions.

## 6 Acknowledgements

The research is conducted in the National Competence Centre of Research (NCCR) Digital Fabrication funded by the SNSF at ETH Zürich. The authors thank Heinz Richner, Andi Reusser, Michael Lyrenmann, Philippe Fleischmann, Bruno Pinto Aranda for technical assistance and Alan Colmant, Marius Graf, Nicolas Neff for their experimental work providing the base of this paper with their Bachelor thesis.

## References

- [1] I. Agustí-Juan, F. Müller, N. Hack, T. Wangler, G. Habert: Potential benefits of digital fabrication for complex structures: Environmental assessment of a robotically fabricated concrete wall. *Journal of Cleaner Production*. (2017) 330–340.
- [2] T. Wangler, E. Lloret-Fritschi, L. Reiter, N. Hack, F. Gramazio, M. Kohler, M. Bernhard, B. Dillenburger, J. Buchli, N. Roussel, R. Flatt: Digital Concrete: Opportunities and Challenges. *RILEM Tech Lett.* 1. (2016) 67.
- [3] A. Szabo, E. Lloret-Fritschi, L. Reiter, F. Gramazio, M. Kohler, R.J. Flatt: Revisiting Folded Forms with Digital Fabrication. In: *Proceedings of eCAADe SIGraDi*, (2019) 191–200.
- [4] E. Lloret-Fritschi, T. Wangler, L. Gebhard, J. Mata-Falcón, S. Mantellato, F. Scotto, J. Burger, A. Szabo, N. Ruffray, L. Reiter, F. Boscaro, W. Kaufmann, F. Gramazio, M. Kohler, R.J. Flatt: From Smart Dynamic Casting to a growing family of Digital Casting Systems. Submitted to: *CCR Special Issue: Digital Concrete 2020*.
- [5] E. Lloret-Fritschi, A.R. Shahab, M. Linus, R.J. Flatt, F. Gramazio, M. Kohler, S. Langenberg: Complex concrete structures: Merging existing casting techniques with digital fabrication. *CAD Computer Aided Design*. (2015) 40–49.
- [6] E. Lloret-Fritschi, L. Reiter, T. Wangler, F. Gramazio, M. Kohler, R.J. Flatt: Slipforming with Flexible Formwork - Inline Measurement and Control. In: *Second Concrete Innovation Conference*, (2017).
- [7] L. Reiter, T. Wangler, N. Roussel, R.J. Flatt: Continuous characterization method for structural build-up. In: *RheoCon2 Conference and SCC9 Symposium*, (2019).
- [8] A.-M. Anton, P. Bedarf, A. Yoo, L. Reiter, T. Wangler, B. Dillenburger, Concrete Choreography: Prefabrication of 3D Printed Columns. In: *Proceedings Fabricate*, (2020).
- [9] A. Szabo, L. Reiter, E. Lloret-Fritschi, F. Gramazio, M. Kohler, R.J. Flatt: Processing of Set on Demand Solutions for Digital Fabrication in Architecture. In: *Proceedings of RheoCon2 Conference and SCC9 Symposium*, (2019) 440–447.
- [10] A. Hajiesmaeili, E. Denarié: Next generation UHPFRC for sustainable structural applications. in: *DSCS 2018: 2nd International Workshop on Durability and Sustainability of Concrete Structures*, (2018).
- [11] A. Szabo, L. Reiter, E. Lloret-Fritschi, F. Gramazio, M. Kohler, R.J. Flatt: Adapting Smart Dynamic Casting to Thin Folded Geometries. in: T. Wangler, R.J. Flatt (Eds.), *First RILEM International Conference on Concrete and Digital Fabrication – Digital Concrete 2018*, Springer International Publishing, (2019) pp. 81–93.